Electronic Supplementary Information

A xanthene-based probe with dual reaction sites enables fluorescence turn-on detection of thiophenol in an aqueous medium

Bhanu Priya,[a] Naresh Kumar,*[b] Deepak Mishra[b] and Roopa*[a]

[a]Department of Applied Sciences, I.K. Gujral Punjab Technical University, Kapurthala 144603 Punjab, India

[b]Department of Chemistry, SRM University, Delhi-NCR, Sonepat-131029, Haryana, India

* Corresponding authors.

E-mail addresses: naresh.chem.ia@gmail.com (N. Kumar); dr.roopa@ptu.ac.in (Roopa)

Table S1. Comparison of Xanth-NO_2 with various thiophenol selective fluorescent probes

Probe Structure	Solvent Conditions	Fluorescence based discrimination of PhSH and H_2S	PhSH Detection Limit	Reference
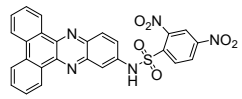	PBS buffer/DMSO; 1 : 1, v/v (50% DMSO)	-	0.04 μM	*RSC Adv.*, 2022, 12, 8611
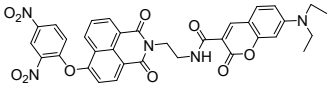	PBS buffer/DMF; 6 : 4, v/v (40% DMF)	-	0.12 μM	*RSC Adv.*, 2015, 5, 94216
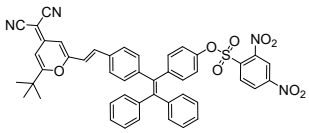	PBS buffer/THF; 9:1, v/v (10% THF)	-	0.0094 μM	*Org. Biomol. Chem.*, 2019, 17, 9251
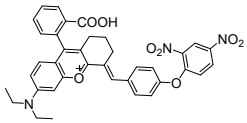	PBS buffer/DMSO; 1 : 1, v/v (50% DMSO)	-	0.120 μM	*New J. Chem.*, 2020, 44, 17360
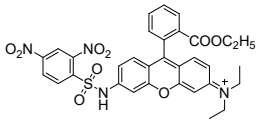	HEPES buffer/DMSO; 1 : 1, v/v (50% DMSO)	-	0.037 μM	*Talanta*, 2018, 181, 239
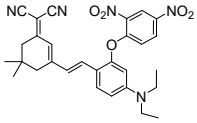	PBS buffer/DMSO; 1 : 1, v/v (50% DMSO)	-	0.034 μM	*Environ. Pollut.*, 2020, 265, 114958
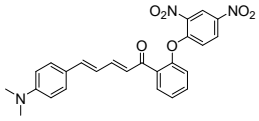	PBS buffer/DMF; 9 : 1, v/v (10% DMF)	-	0.038 μM	*ACS Omega*, 2020, 5, 10808
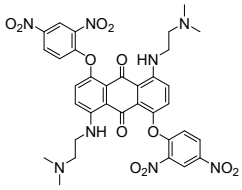	HEPES buffer/DMSO; 7 : 3, v/v (30% DMSO)	-	0.015 μM	*Chem. Commun.*, 2021, 57, 2800
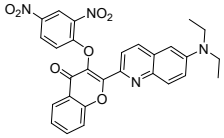	PBS buffer/DMF; 3 : 1, v/v (25% DMF)	-	0.0072 μM	*Dye. Pigment.*, 2021, 190, 109289
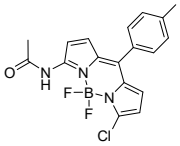	HEPES buffer/CH_3CN 3 :1, v/v (25% CH_3CN)	-	0.0369 μM	*Sensors and Actuators B,* 2017, 252, 470

--*Continue*

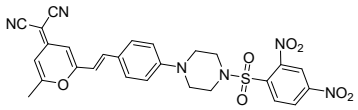	HEPES buffer/DMSO; 7 : 3, v/v (30% DMSO)	-	0.0083 μM	*Analyst*, 2018, 143, 756
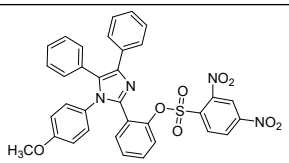	PBS buffer/CH_3CN; 1 : 1, v/v (50% CH_3CN)	-	0.189 μM	*Anal. Methods,* 2016, 8, 1425
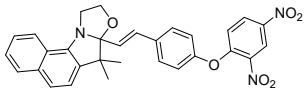	PBS buffer/CH_3CN; 1 : 1, v/v (50% CH_3CN)	-	0.007 μM	*RSC Adv.,* 2017, 7, 46148
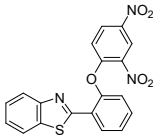	45% DMF in PBS buffer	-	0.03 μM	*RSC Adv.*, 2016, 6, 52790
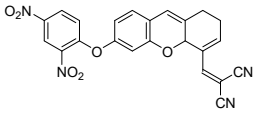	PBS buffer/DMF; 8 : 2, v/v (20% DMF)	-	0.009 μM	*New J. Chem.,* 2019, 43, 14139
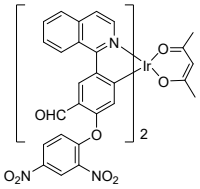	HEPES buffer/CH_3CN; 1 : 1, v/v (50% CH_3CN)	-	0.0038 μM	*Analytical Chemistry*, 2019, 91, 1353
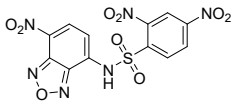	**Phosphate buffer**	**-**	**20 μM**	*Angew. Chem. Int. Ed.*, 2007, 46, 8445
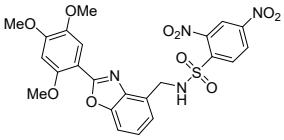	**Phosphate buffer**	**-**	**0.2 μM**	*Chem. Commun.*, 2010, 46, 1944
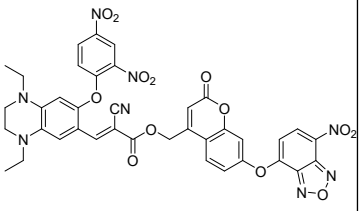	PBS buffer/CH_3CN; 7 : 3, v/v (30% CH_3CN)	The probe exhibits similar reactivity for H_2S and glutathione, making no clear discrimination between PhSH and H_2S	0.34 μM	*ACS Sens.*, 2018, 3, 1863
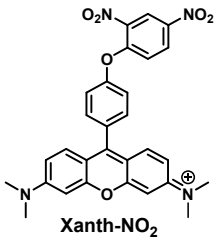 **Xanth-NO_2**	**HEPES buffer/DMSO; 9.75 : 0.25, v/v (2.5% DMSO)**	**Xanth-NO_2 reacted differently with PhSH and H_2S, allowing to distinguish between these two analytes.**	**0.13 μM**	**This Work**

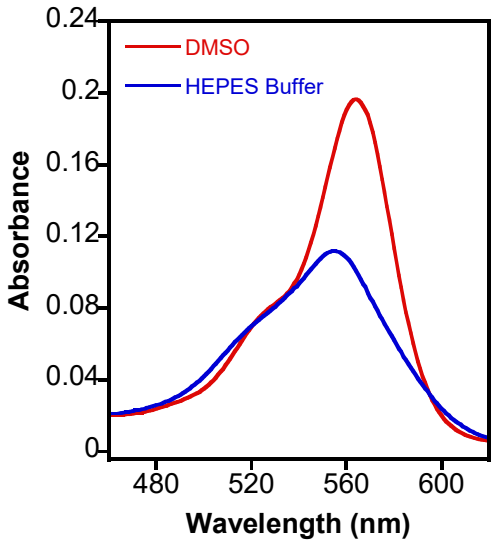

Fig. S1: Absorption spectra of Xanth-NO_2 (5 μM) in DMSO and HEPES buffer (pH 7.4) containing 2.5% DMSO.

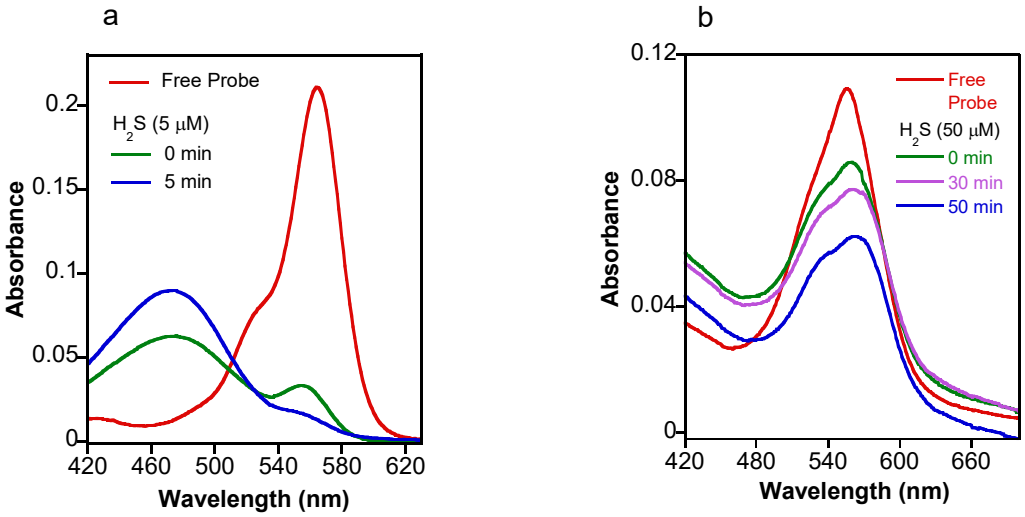

Fig. S2: Absorption spectra of Xanth-NO_2 (5 μM) with H_2S as Na_2S in: (a) DMSO and (b) HEPES buffer (pH 7.4) containing 2.5% DMSO.

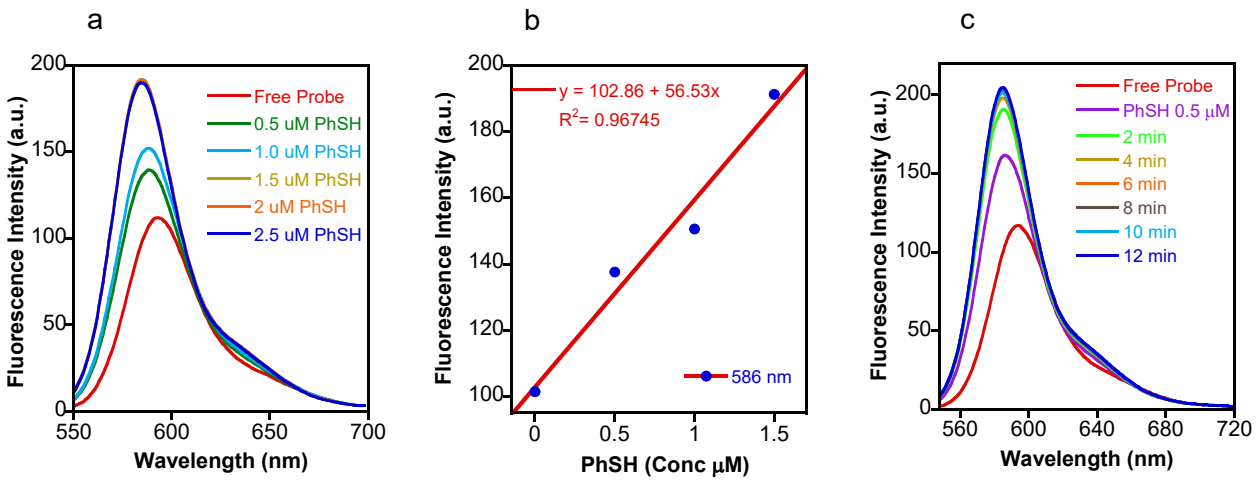

Fig. S3: (a) Fluorescence response of Xanth-NO_2 (5 μM) with increasing concentrations of PhSH. (b) Plot of a linear relationship between the fluorescence intensity at 586 nm and the concentration of PhSH. (c) Time-dependent fluorescence change of Xanth-NO_2 in the presence of PhSH. The experiments were performed in DMSO at 25 °C, λ_{ex} = 540 nm.

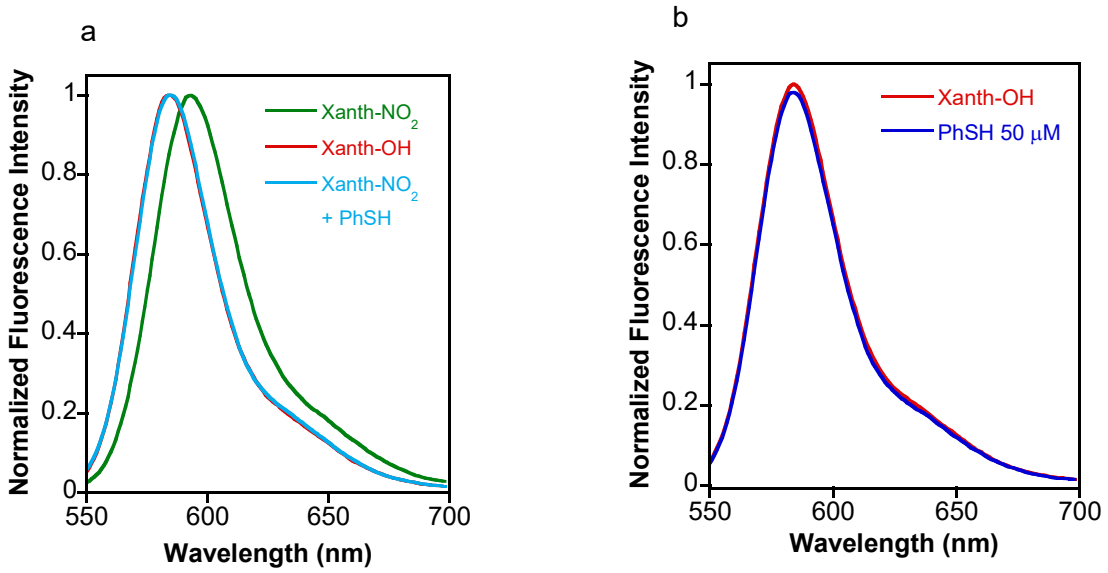

Fig. S4: Normalized fluorescence of: (a) Xanth-NO_2, Xanth-OH and Xanth-NO_2 + PhSH; (b) Xanth-OH with and without PhSH. Conditions: Solvent: DMSO, 25 °C, λ_{ex} = 540 nm.

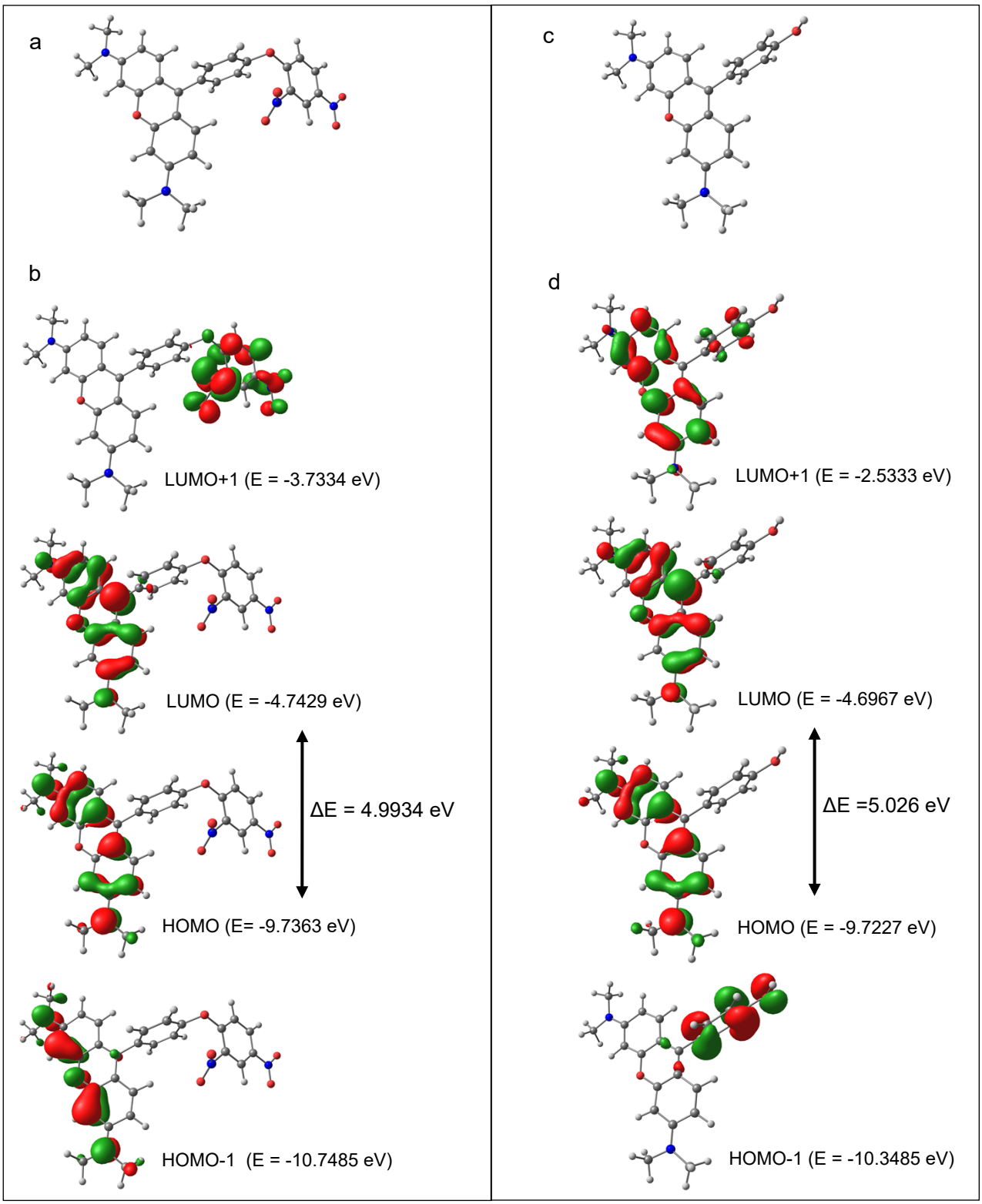

Fig. S5: Optimized structures of Xanth-NO_2 (a) and Xanth-OH (c). Molecular orbitals and energies of Xanth-NO_2 (b) and Xanth-OH (d) using gas phase TD-DFT calculations based on the CAMB3LYP/TZV basis set level.

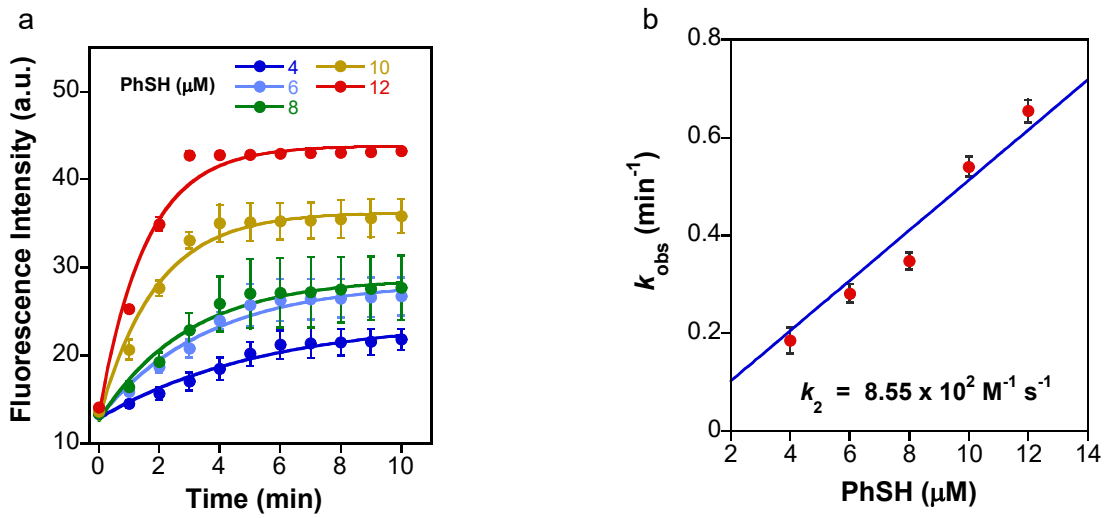

Fig. S6: Rate constant evaluation: (a) Time course of reaction of Xanth-NO_2 (0.2 μM) using different concentrations of PhSH in HEPES buffer (pH 7.4) containing 2.5% DMSO at 25 ºC; $\lambda_{ex/em}$ 540/571 nm. (b) Plot of observed rate constant (k_{obs}) as a function of PhSH concentrations. Error bars denote the standard deviation, SD, and n = 3.

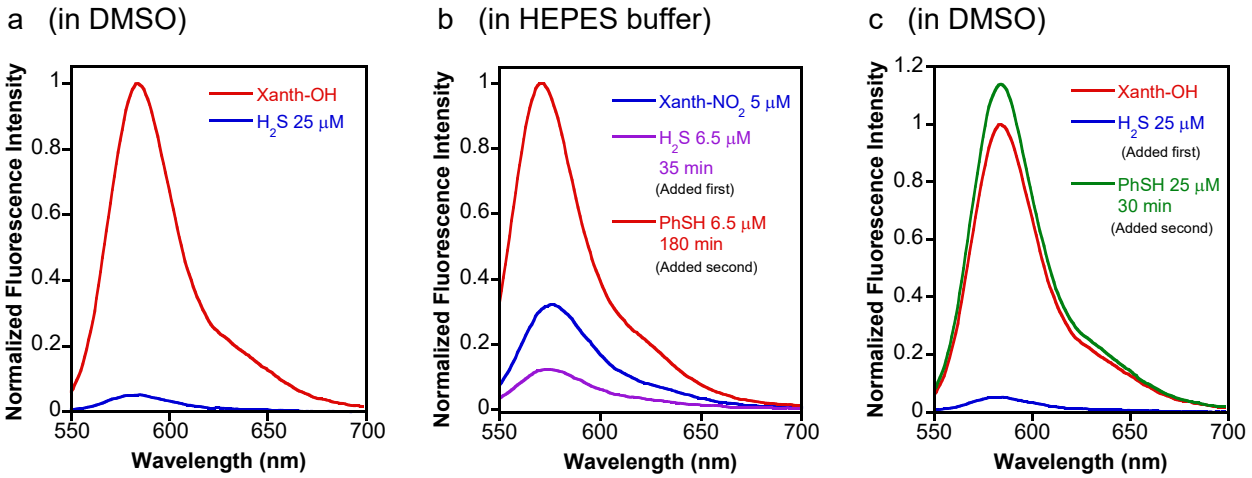

Fig. S7: Normalized fluorescence intensity of: (a) Xanth-OH with and without H_2S; (b) Xanth-NO_2 and (c) Xanth-OH upon sequential addition of H_2S and PhSH. For a and c, data reported in DMSO, 25 ºC; λ_{ex} 540 nm; For b, data reported in HEPES buffer (pH 7.4) containing 2.5% DMSO at 25 ºC, λ_{ex} = 540 nm.

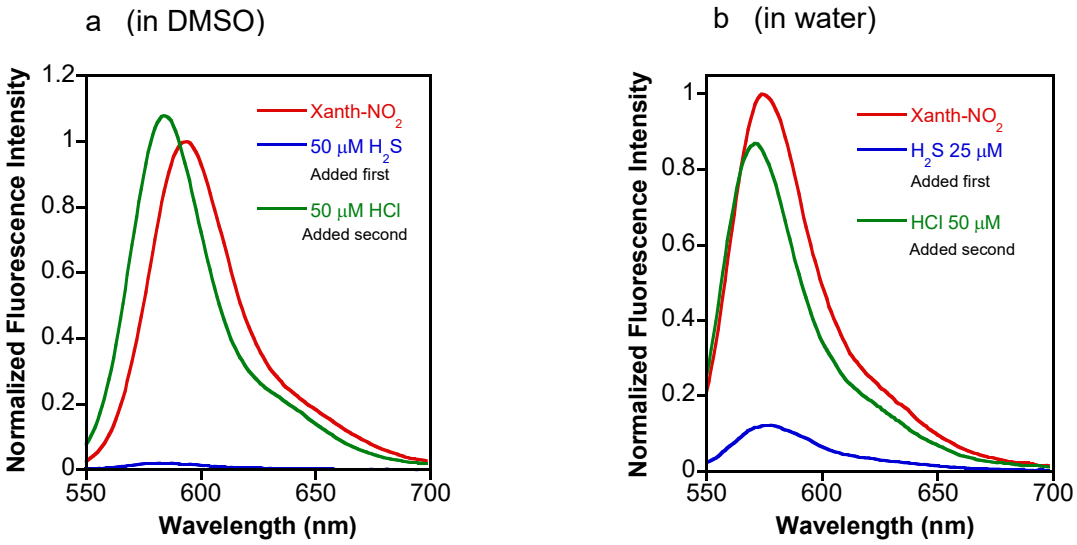

Fig. S8: Normalized fluorescence intensity of Xanth-NO_2 upon sequential addition of H_2S and HCl. (a) In DMSO; (b) In water containing 2.5% DMSO. Data reported at 25 ºC; λ_{ex} 540 nm.

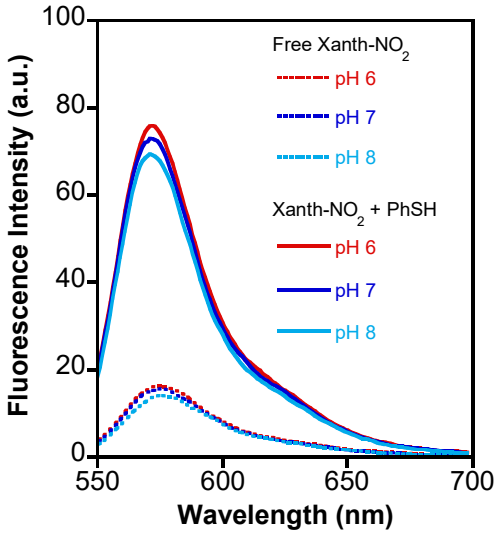

Fig. S9: Fluorescence profile of Xanth-NO_2 (5 μM) without or with PhSH (10 μM) under different pH environments. The pH was adjusted by adding aqueous NaOH or HCl. Data reported immediately after the addition of PhSH in water containing 2.5% DMSO at 25 ºC; λ_{ex} 540 nm.

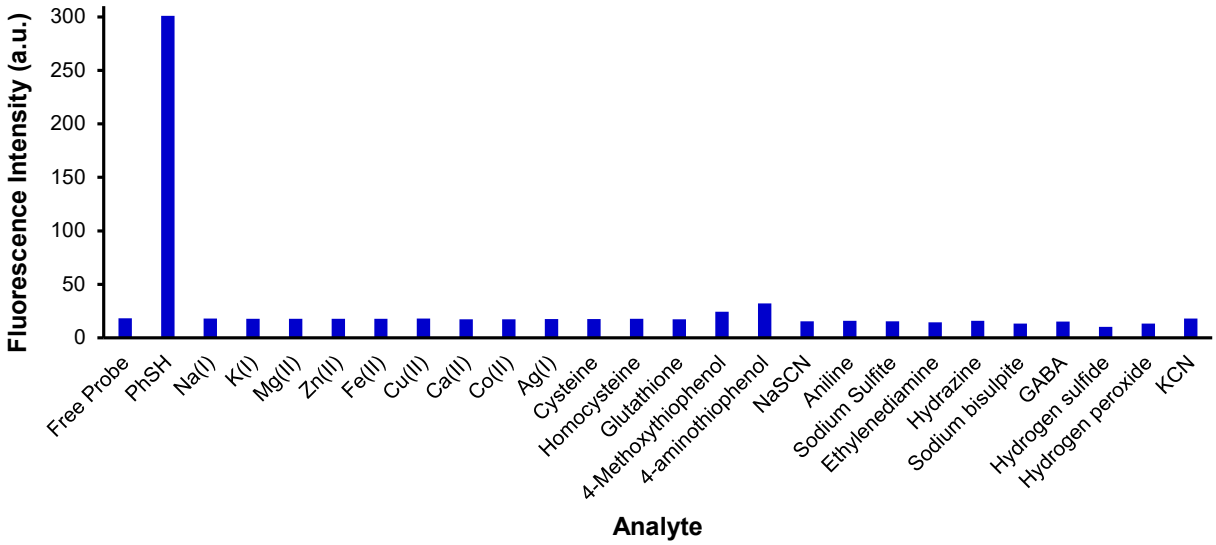

Fig. S10: Selectivity profile of Xanth-NO_2 (5 μM) with different analytes (20 μM in each case). Data reported after 5 min of addition in HEPES buffer (pH 7.4) containing 2.5% DMSO at 25 ºC; $\lambda_{ex/em}$ 540 nm/571 nm.

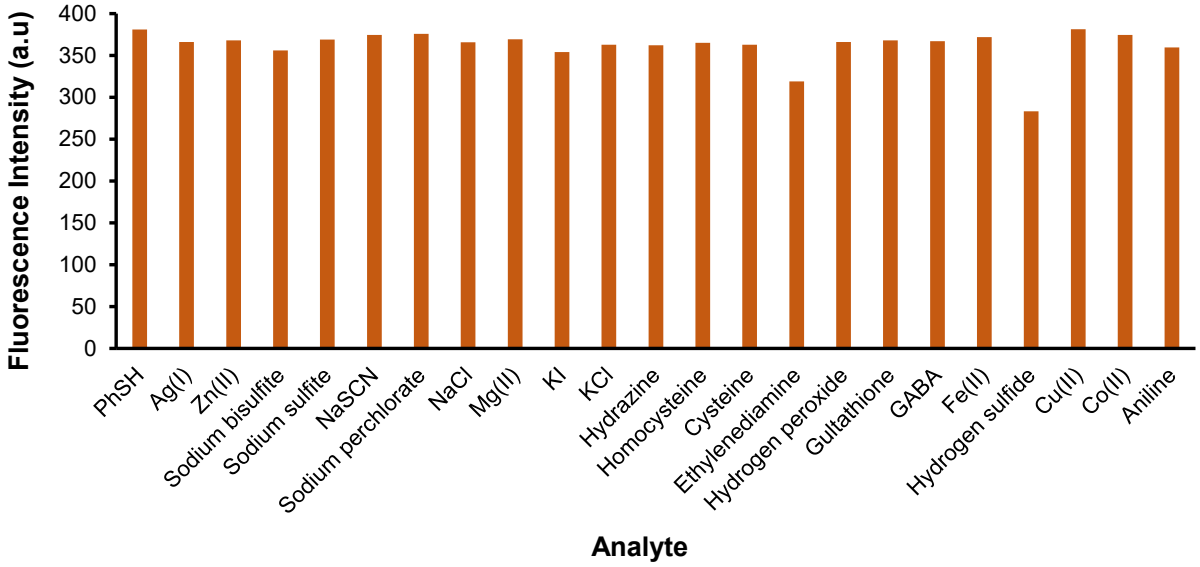

Fig. S11: Competitive selectivity profile of Xanth-NO_2 (5 μM) for PhSH in presence of different analytes. Data reported after 10 min of addition in HEPES buffer (pH 7.4) containing 2.5% DMSO at 25 ºC; $\lambda_{ex/em}$ 540 nm/571 nm.

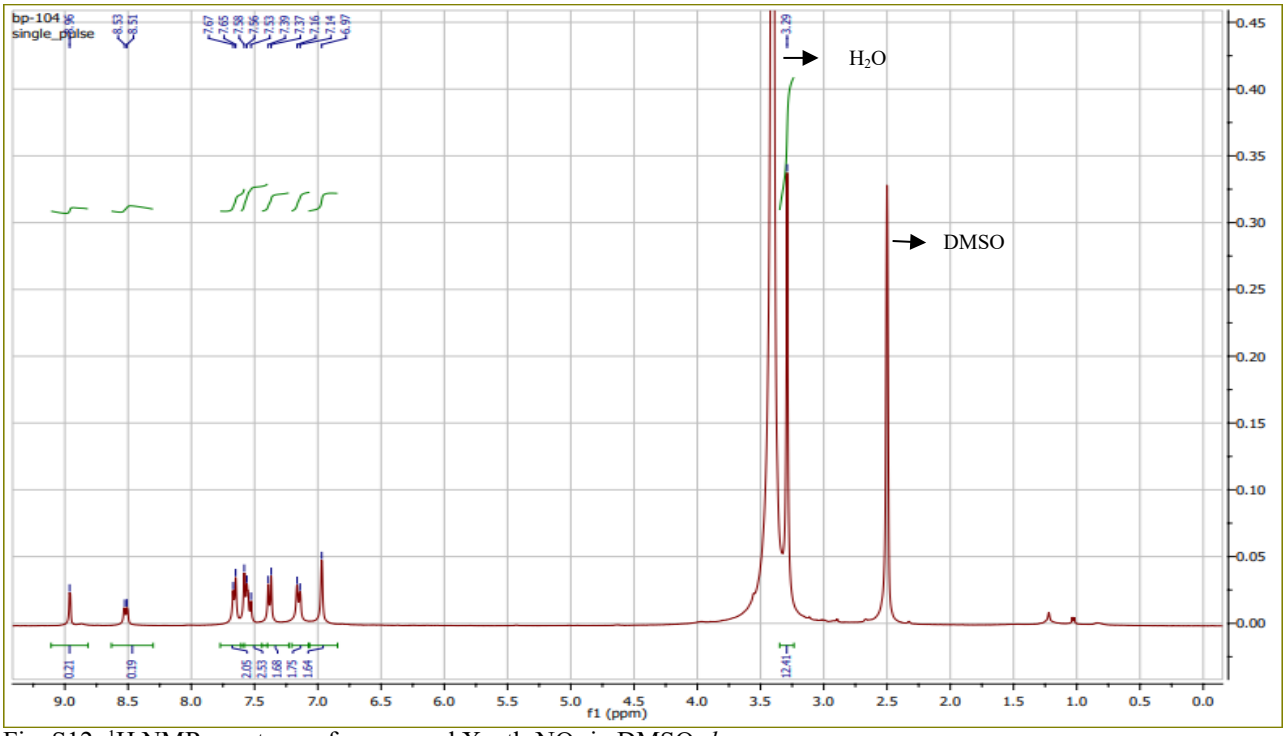

Fig. S12: ^{1}H NMR spectrum of compound Xanth-NO_2 in DMSO-d_6.

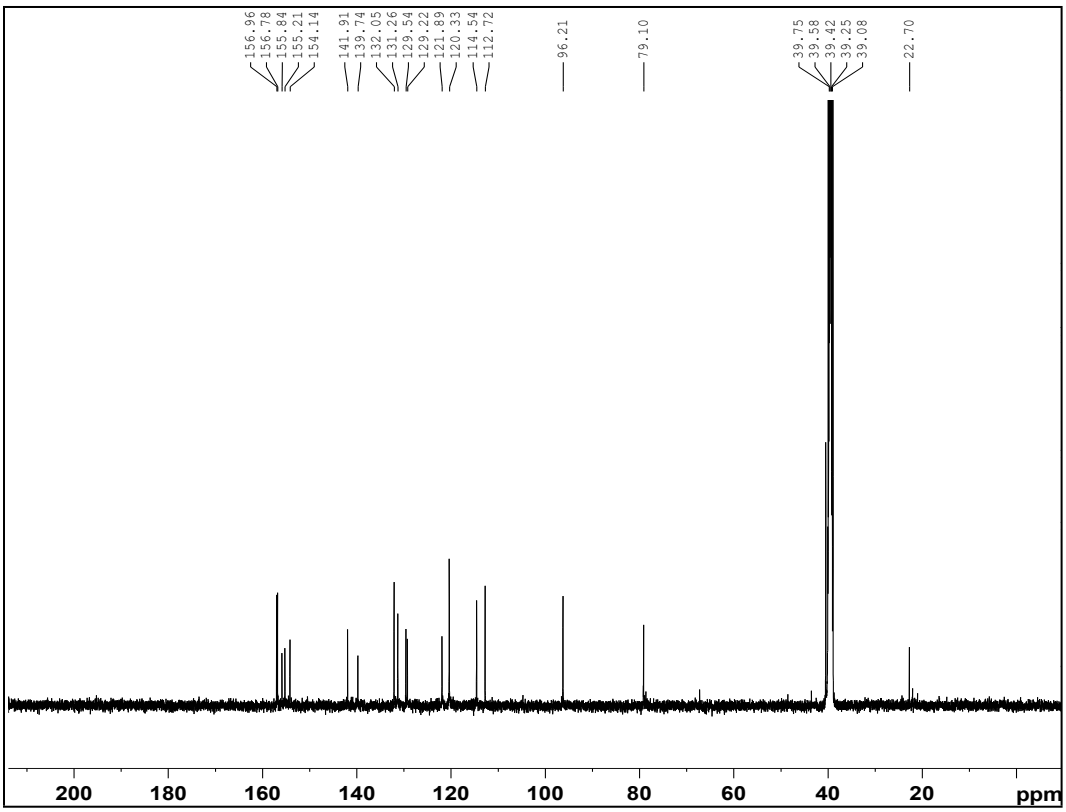

Fig. S13: ^{13}C NMR spectrum of compound Xanth-NO_2 in DMSO-d_6.

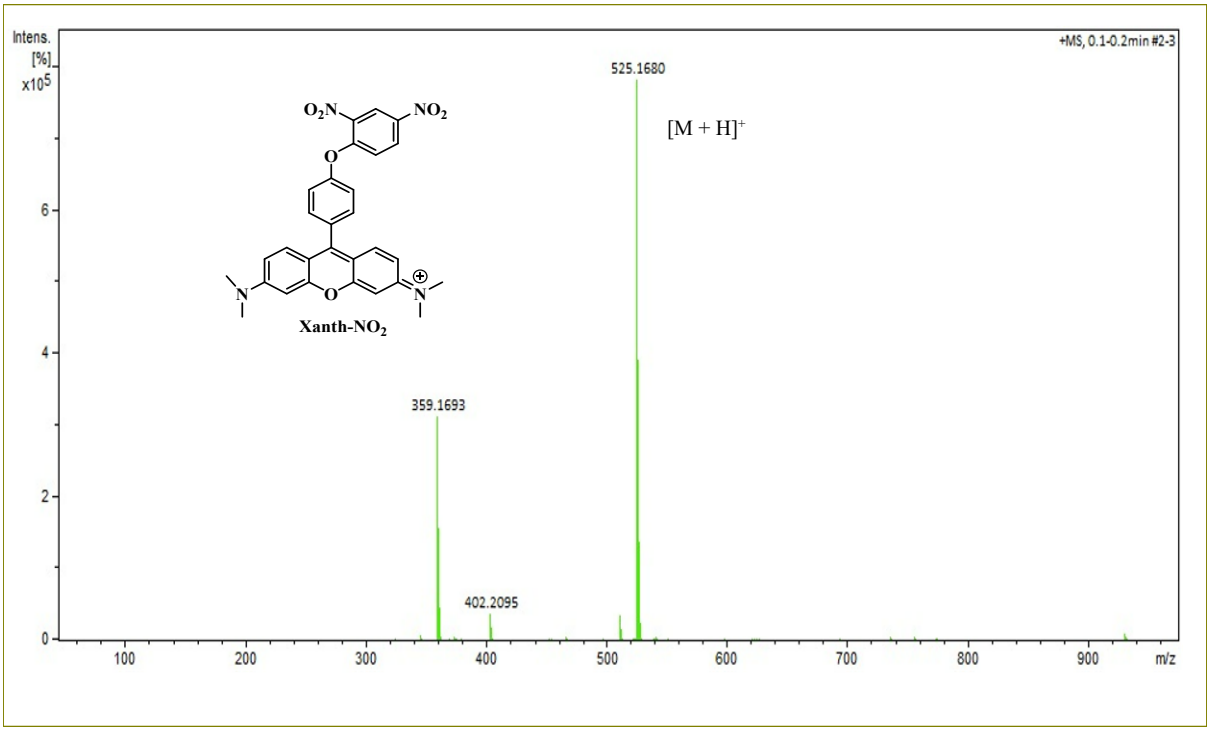

Fig. S14: HRMS spectrum of compound Xanth-NO_2.

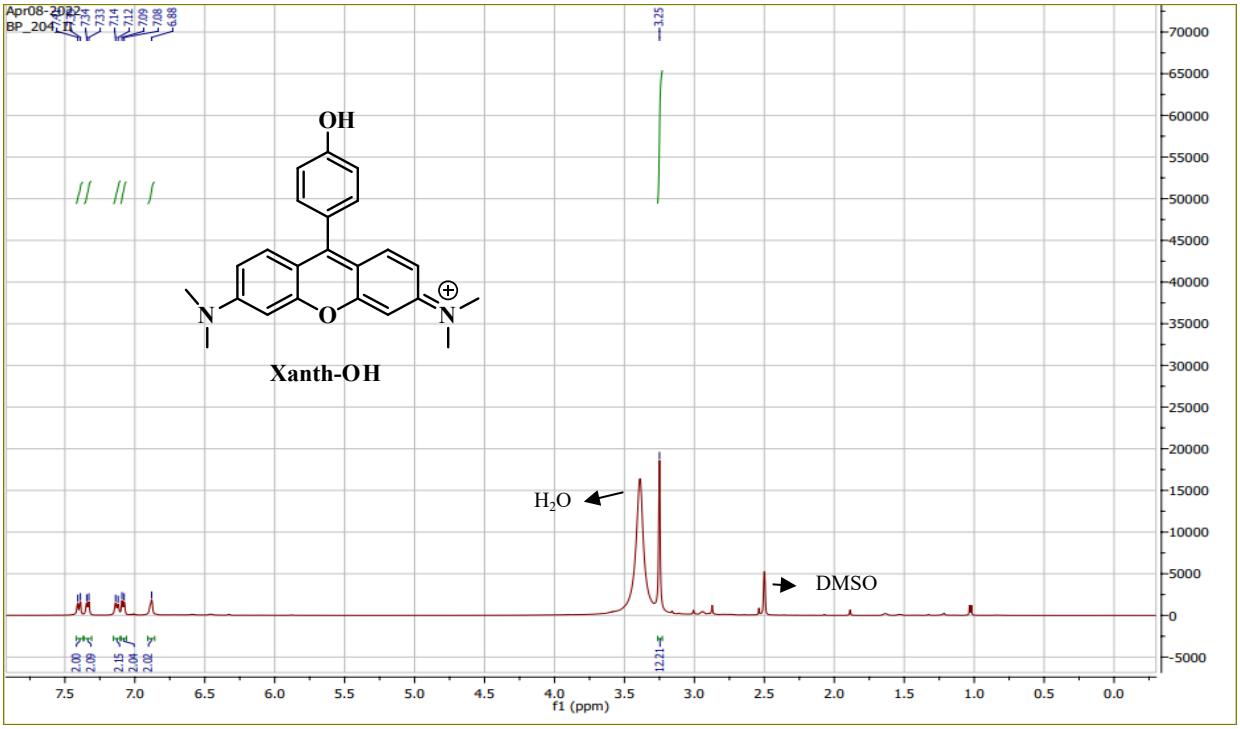

Fig. S15: ^{1}H NMR spectrum of compound Xanth-OH in DMSO-d_6

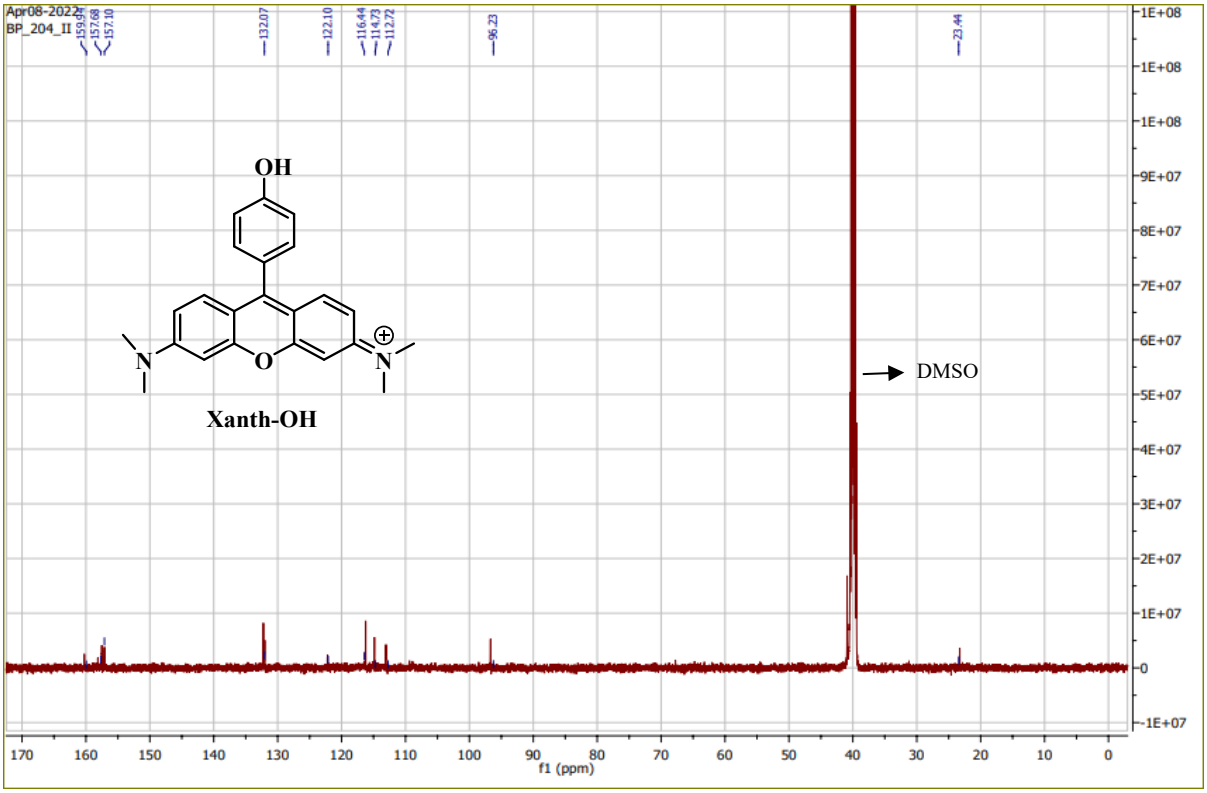

Fig. S16: ^{13}C spectrum of compound Xanth-OH in DMSO-d_6.

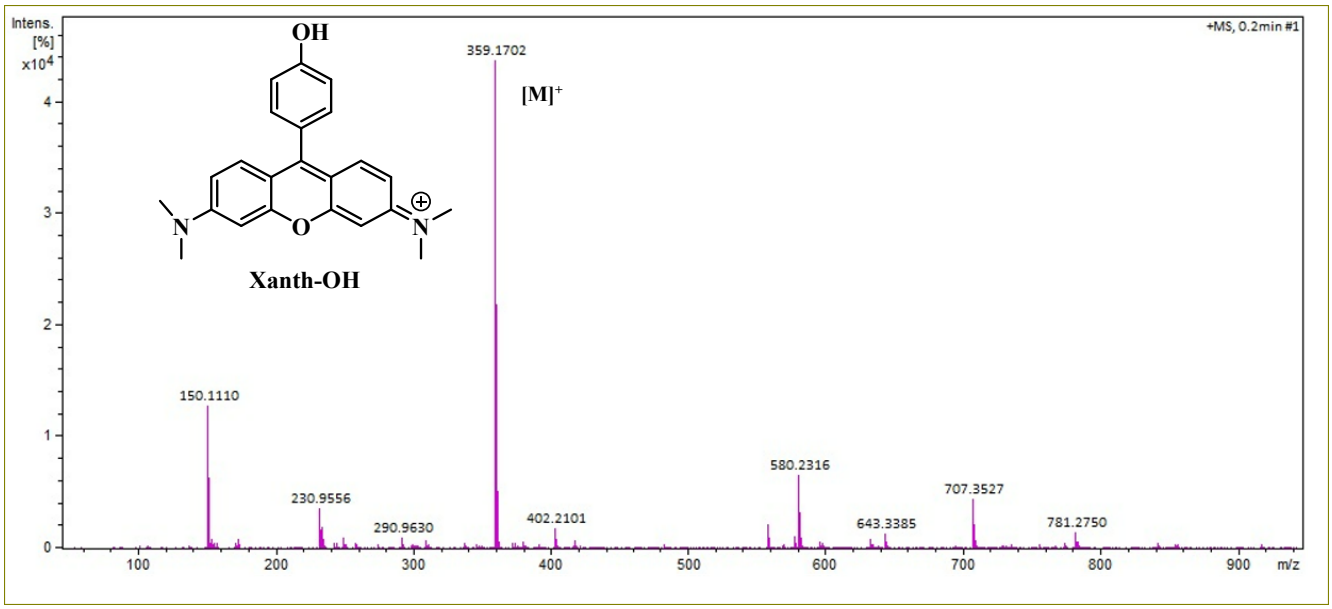

Fig. S17: HRMS spectrum of compound Xanth-OH.

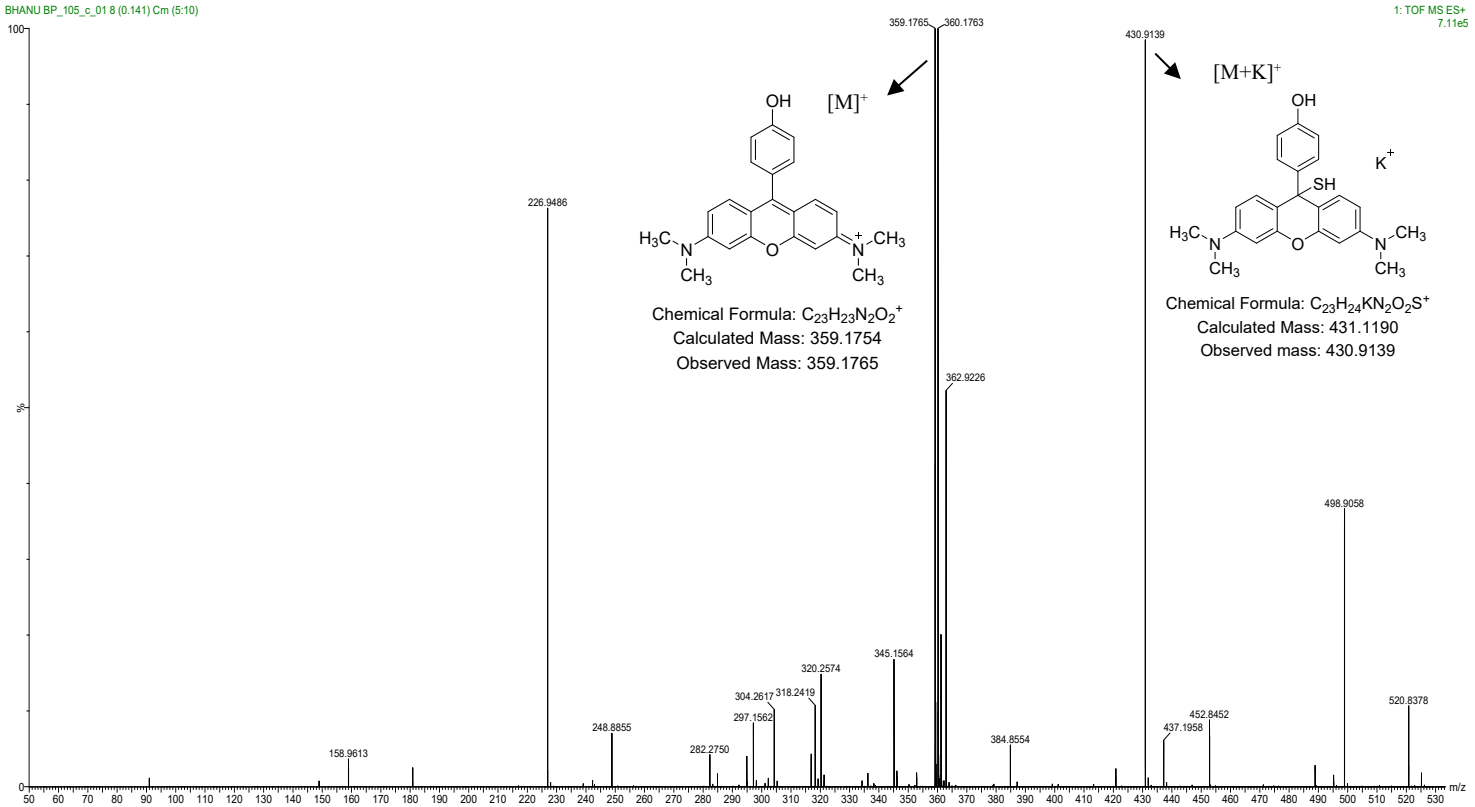

Fig. S18: Mass spectrum of compound Xanth-NO_2 in the presence of H_2S.

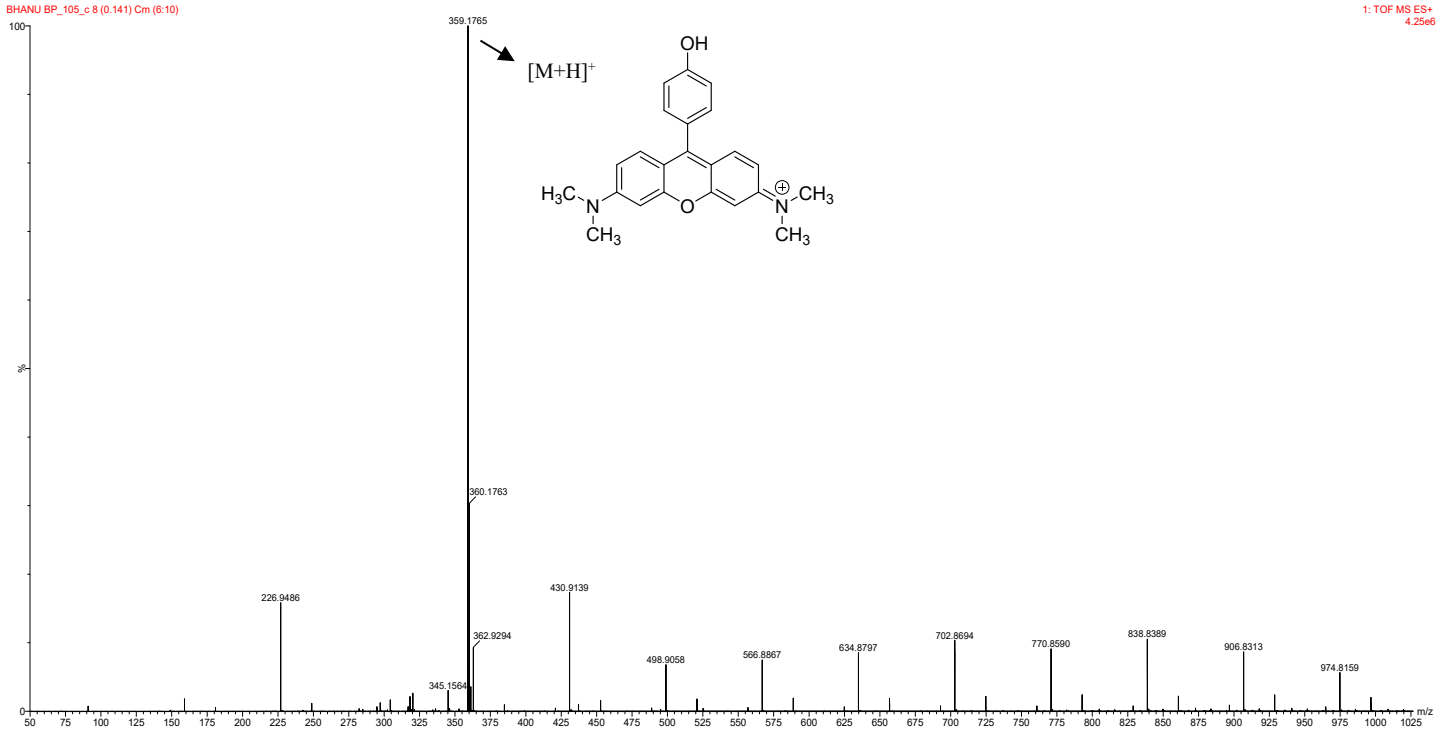

Fig. S19: Mass spectrum of compound Xanth-NO_2 with the addition of PhSH.

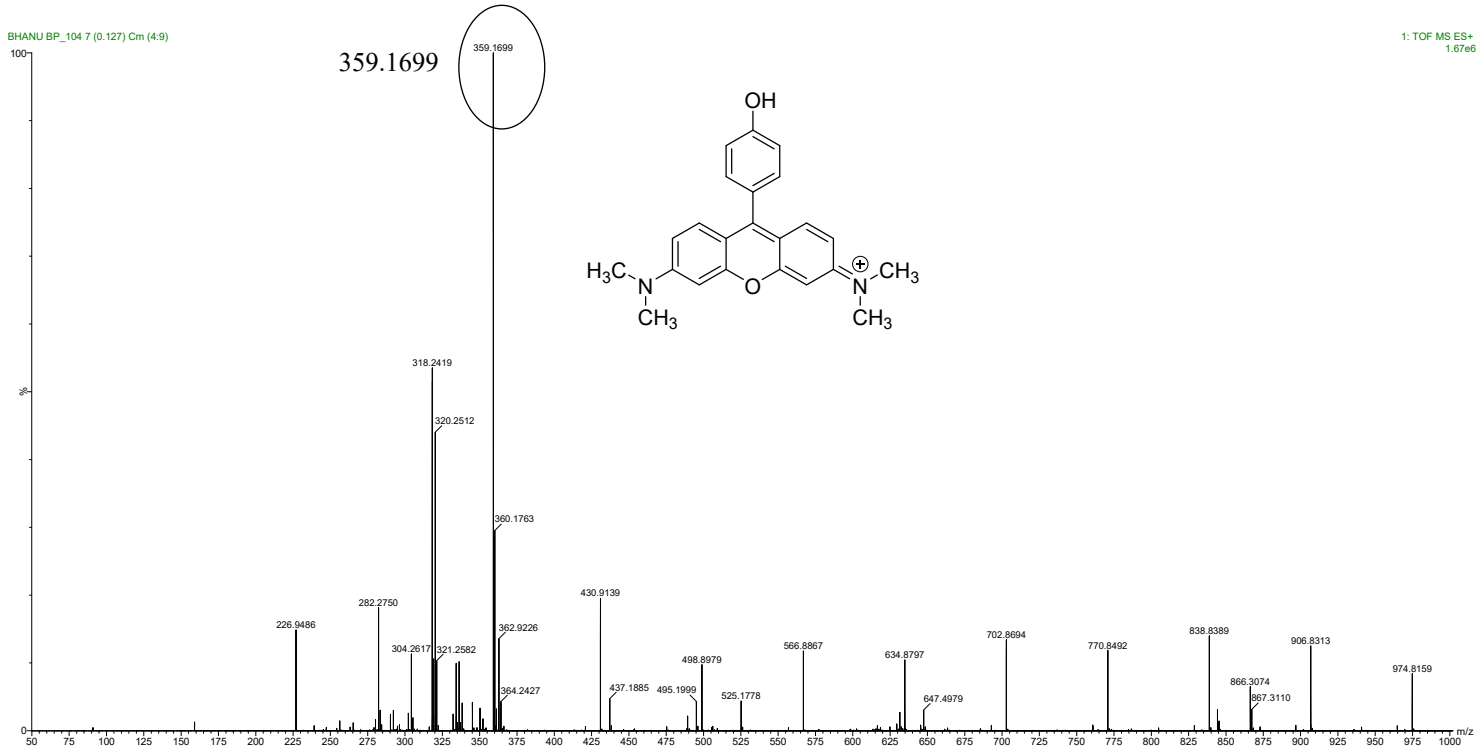

Fig. S20: Mass spectrum of compound Xanth-NO_2 with the addition of H_2S and further addition of PhSH.